Raman *in Vivo* Analysis of Melanoma Invasion Level

Lyudmila A. Bratchenko[1*], Yulia A. Khristoforova[1], Yulia G. Loginova[2], Alexander A. Moryatov[2], Valery P. Zakharov[1], Oleg I. Kaganov[2], and Ivan A. Bratchenko[1]

[1] Department of Laser and Biotechnical Systems, Samara National Research University, 34 Moskovskoe Shosse, Samara 443086, Russian Federation

[2] Department of Oncology, Samara State Medical University, 89 Chapaevskaya str., Samara 443099, Russian Federation

*e-mail: shamina94@inbox.ru

Abstract. The number of diagnosed melanoma cases is increasing every year, and there is an urgent need for novel screening approaches that may help in the diagnosis and prognosis of melanoma. In this study we propose to utilize conventional Raman spectroscopy for the determination of Clark level of invasion. We collected spectral data from 59 melanoma samples and achieved accuracy of 75% for discrimination of I–II vs. III–V levels of invasion. This study is the first to explore the potential of spectral analysis, utilizing Raman scattering and autofluorescence techniques, for distinguishing melanoma tissues according to their invasion level. Analysis of spectral data was performed with the application of projection on latent structures and discriminant analysis. The most significant for the model is the spectrum bands, associated with autofluorescence. The most informative bands of the Raman component for the constructed discrimination of melanoma tissues by the degree of invasion are the bands of 1385 cm^{-1}, 1445 cm^{-1}, 1487 cm^{-1}, 1565 cm^{-1}, and 1695 cm^{-1}, associated with the presence of pigments (melanin), protein components (e.g., amide bonds, collagen), and lipid structures. The proposed approach may be useful in fast screening analysis for the determination of the best treatment plan for the patient based solely on the analysis of Raman spectra.

Keywords: Clark level; melanoma; Raman spectroscopy; autofluorescence; optical biopsy; invasion, PLS.

Paper #9324 received 18 Aug 2025; revised manuscript received 27 Aug 2025; accepted for publication 27 Aug 2025; published online 30 Sep 2025. doi: 10.18287/JBPE25.11.030303.

1 Introduction

The number of diagnosed melanoma cases is increasing every year, and there is an urgent need for novel screening approaches that may help in the diagnosis and prognosis of melanoma [1]. One of the most common approaches to evaluate the stage of melanoma growth and further evaluate a patient's prognosis is a Clark level. The Clark level of invasion is determined by examining the depth of melanoma's penetration into the skin's layers during a microscopic study. It categorizes the melanoma's spread into five levels (I–V), ranging from the epidermis to the subcutaneous tissue. A pathologist, examining the tissue, uses this information to assess the melanoma's stage and prognosis [2].

Since 1969 Clark and his collaborators had found a link between the level of tumor invasion and the prognosis of patients with cutaneous melanoma. They showed a median survival time of 6.83 years for the patients with level II of invasion and 3.5 years for level V [3, 4]. Thus, the information about Clark level of invasion provides an opportunity to predict an outcome for the patient. In this regard, it would be very helpful in medical practice to determine Clark level of invasion fully in noninvasive manner (in contrast to the pathologist examination).

Today there are numerous methods that may be used for skin tissue analysis: ultrasound imaging [5], magnetic resonance imaging [6], optical coherence tomography [7], optoacoustic imaging [8], scanning electron microscopy [9], fluorescence lifetime imaging [10], and many others. Despite the capabilities of the mentioned approaches, there are several limiting factors that prevent the inclusion of such technologies in medical practice. Such limitations include the high price of equipment

(magnetic resonance imaging, fluorescence lifetime imaging, optoacoustic imaging), very limited depth of analysis (optical coherence tomography), low resolution (ultrasound imaging), etc. [11]. The described methods utilize information about tumor invasion; however, there is an opportunity to measure the chemical composition of the tumor and predict the invasion level based on this information.

One possible way to create a simple and reliable method of tissue noninvasive component analysis is the application of Raman spectroscopy (RS) [12]. RS may provide fast and reliable data about skin tissue composition [13] and offers an opportunity to create handheld portable devices [14]. Application of RS (and its modifications) was mainly demonstrated for the precise diagnosis of skin tumors (both *ex vivo* and *in vivo* [15]); however, application of RS in the determination of the Clark level of invasion was never investigated.

In this study we investigate a possibility to determine Clark level of invasion based solely on the analysis of Raman spectra from the analyzed melanoma tissues. We aimed at differentiation of Clark level I and II melanomas from Clark level III, IV and V. We analyzed *in vivo* melanomas with a portable Raman device and utilized well-known machine learning techniques for the classification of melanoma level of invasion and utilized validation techniques to guarantee the robustness of the proposed approach.

2 Materials and Methods

2.1 Melanoma Tissue Samples and Experiment Preparation

In the current study, *in vivo* analysis of melanoma tissues was performed at the Samara Regional Clinical Oncology Dispensary. Patients were selected using stratified random sampling. The study included 59 people. All subjects were Caucasian with skin phototypes I and II. The Clark invasion level was established based on the histological examination results. The characteristics of the study sample are presented in Table 1. Standardized *in vivo* registration of spectral characteristics of melanoma tissue was performed for each patient. Informed consent was obtained from the patients; all participants were over 18 years of age. The *in vivo* study protocols were approved by Samara State Medical University (Samara Region, Samara, Russia, protocol No 132, 29 May 2013, and clinical studies fall within the Code of Ethics of a Doctor of Russia, approved at the 4th conference of the Russian Medical Association, and within the World Medical Association Declaration of Helsinki).

Table 1 Brief description of the sample.

Group	Clark level	Number of patients	Number of spectra
1	1, 2	26	26
2	3, 4, 5	33	33

2.2 Experimental Portable Raman System

Excitation of Raman scattering spectra of melanoma tissues was performed using a laser module (LuxxMaster LML-785.0RB-04, PD-LD, New Jersey, USA) with a central wavelength of 785 nm. The Raman probe (RPB785, InPhotonics, Massachusetts, USA) focuses the excitation radiation and collects and filters the scattered radiation. The focal length of the Raman probe used was 7.5 mm. A tip with a silicone attachment was used to fix the distance of 7 mm between the probe and the melanoma tissue surface, which made it possible to collect scattered light from the upper layers of the skin (up to 1–2 mm deep). The laser power density on the melanoma tissue surface was about 0.3 W/cm^2 and did not cause damage or discomfort to patients. The collected signal was decomposed into a spectrum using a portable spectrometer (QE65Pro, Ocean Optics, Florida, USA). Spectra were recorded in the range of 800–914 nm with a spectral resolution of 0.2 nm and an exposure time of 20 s with 3 accumulations.

2.3 Processing and Analysis of Experimental Data

The spectra were recorded using the SpectraSuite program (Ocean Optics, Florida, USA). Immediately before recording the spectral characteristics of the studied samples, a preliminary registration of the background signal of the system without a melanoma tissue sample was performed. After that, the background component was automatically subtracted from the subsequent recorded skin spectra using the built-in SpectraSuite algorithm. Each of the obtained spectra is a discrete set of 455 parameters (predictors).

The experimental data are characterized by multicollinearity, high fluorescent background, and multiple overlaps of the spectral contribution of various components of melanoma tissue. Bilinear and nonlinear methods of analysis have proven themselves well for solving the task of discrimination of such spectral data of multicomponent biological samples [16−18]. It should be noted that the analyzed sample has a limited volume of patients with a large number of parameters for each patient. Therefore, the use of nonlinear machine learning methods is complicated by the risk of overfitting the model and is undesirable for the current sample. In the current work, projection bilinear methods are advisable to use to achieve a statistically reliable result. Therefore, the experimental data were subjected to discriminant analysis with projection onto latent structures (PLS-DA). PLS-DA models were constructed using the MDAtools package available within the R studio software [19]. Thus, the work solves the task of supervised classification, where each patient in the sample is characterized by spectral data (parameter matrix) and a priori information about belonging to a group depending on the degree of melanoma invasion (target data vector). In conditions of a limited sample size and a large number of parameters for each patient, it is necessary to strictly control the overfitting of the model to avoid

overestimated discrimination characteristics. Previously, our research group used a combination of the following to achieve a statistically reliable assessment of the feasibility of the analysis method on a limited sample: 1) control of the standard error of the model during cross-validation; 2) several iterations of building and testing the model, followed by averaging of the characteristics; 3) analysis of important variables for the model [20]. Similarly, in the current work, the spectral dataset was divided randomly: 80% of the samples from each group were used to train the model (training set), and 20% of the samples from each group were used to test the model (test set). Then, the training and test sets were preprocessed. Separate preprocessing eliminates the "leakage" of information about the test set into the model. The spectral data were smoothed using the Savitzky-Golay filter (15 filter window width, 1 order of polynomial used for smoothing, and 0 order of derivative to take) and normalized by the Standard Normal Variate (SNV) algorithm. Smoothing using the Savitzky-Golay filter reduces noise and random fluctuations in the spectral data while preserving important spectral features (peaks and their shapes). Normalization using the SNV method eliminates variations in the spectral intensity caused by external factors not related to the chemical composition. Together, these preprocessing methods provide a more accurate and reliable extraction of informative features of the spectra for subsequent statistical analysis and classification. The PLS-DA model was trained on the training set and then used to classify the test set. In total, random partitioning into training and test sets was repeated 10 times. The number of loading vectors in the model construction was selected in accordance with the first local minimum on the model mean square error graph calculated for a different number of components and k-fold cross-validation predictions (k = 6). The analysis of the most significant spectral bands for the constructed models was implemented based on the variable importance distribution in the constructed projection (VIP distribution) [21]. The VIP distribution allows for determination which spectral ranges have the most significant effect on the prediction of the target variable. The allocated spectral ranges demonstrate those areas of the spectrum that are most responsible for variations in the target variable, which helps to understand the chemical or physical properties of the samples.

3 Results and Discussion

Figure 1 demonstrates the mean pre-processed spectra of melanoma tissues characterized by invasion to the papillary dermis (group 1) and melanoma tissues with invasion to the subcutaneous fat (group 2).

Figure 1 shows that the spectral region of 450–1800 cm^{-1} is characterized by two key components: a broadband autofluorescence signal and weak Raman scattering peaks. To date, a number of scientific groups have demonstrated that the combination of Raman scattering and autofluorescence allows for obtaining comprehensive information on the molecular and metabolic state of skin tissues and skin neoplasms [15, 22, 23]. In the recorded spectra in the range of 450–1200 cm^{-1}, autofluorescence dominates and overlaps the weak Raman signal, which limits the analysis of this range to only the fluorescence characteristics of melanoma. Autofluorescence of human skin in the near-IR range is caused by the presence of various fluorophores, such as collagen, elastin, and melanin. Melanoma demonstrates unique fluorescent properties associated with an increased melanin content and oxidative stress [24–27]. At the same time, in the spectral range of 1200–1800 cm^{-1}, the contribution of autofluorescence decreases, which allows for a clearer resolution of Raman peaks. The recorded spectra of melanoma tissues are characterized by the presence of Raman peaks at 1285 cm^{-1}, 1445 cm^{-1}, and 1665 cm^{-1}. It should be noted that the assignment of spectral bands in the spectrum of melanoma tissue to specific substances is quite complex due to the possible spectral contribution of several substances to one specific band. In an earlier work of our research group, a statistically significant relationship was found between the Raman intensity of the spectral regions 1270–1340, 1440–1460, 1540–1560, and 1640–1670 cm^{-1} and the tumor type [14]. In addition, according to the results of the histological examination, the analyzed melanoma tissue samples are characterized by the presence of lymphoid infiltration of varying severity, which can also make a spectral contribution to the recorded melanoma tissue spectra in the bands 1242–1252, 1450, and 1580–1660 cm^{-1} [28, 29]. Thus, the spectral range of 400–1800 cm^{-1} reflects the combination of autofluorescence and Raman spectral features, which provides a comprehensive approach to the study of melanoma tissue. A strong overlap of the spectra of the analyzed groups should be noted. Weak intergroup dispersion makes it difficult to detect spectral differences between melanoma tissues of different invasions "by eye" and confirms the need to use a multivariate analysis method.

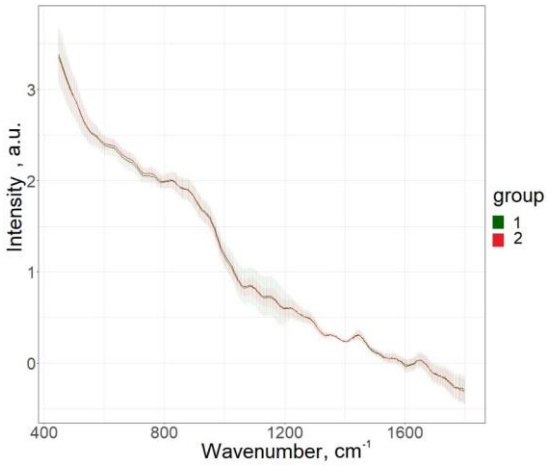

Fig. 1 Mean preprocessed spectra with standard deviation for the group with melanoma invasion from the epidermal layer to the papillary dermis (group 1) and for the group with melanoma invasion to the subcutaneous fat (group 2).

Detection of statistically significant spectral differences in melanoma tissues of different invasions was implemented based on 10 iterations of dividing the spectral base into training and test subsamples with subsequent construction of a PLS-DA model. Figure 2 demonstrates the choice of model parameters using one of the 10 iterations as an example. The distribution of the eigenvalues of the loading vectors demonstrates that the first two loading vectors cover a large share of the explained data variation. At the same time, the model at the iteration under consideration is characterized by a decrease in the mean square error of the model during cross-validation and the absence of a local minimum up to the third loading vector. Thus, for the iteration under consideration of model construction, the 3rd loading vector is optimal, covering the main share of the variation in the original data and not leading to overfitting.

As a result of 10 iterations of model construction, the average characteristics of melanoma tissue discrimination by the degree of invasion for the training data set were: specificity at the level of 0.69, sensitivity 0.67, accuracy 0.68. The average characteristics of the constructed models for the test data were specificity 0.71, sensitivity 0.80, and accuracy 0.75. It should be noted that the models are stable and have good generalization ability, which follows from better indicators of the models for the test sets than for the training ones. The average distribution of the importance of the spectrum variables for 10 iterations of constructing a model of melanoma tissue discrimination by the degree of invasion is shown in Fig. 3.

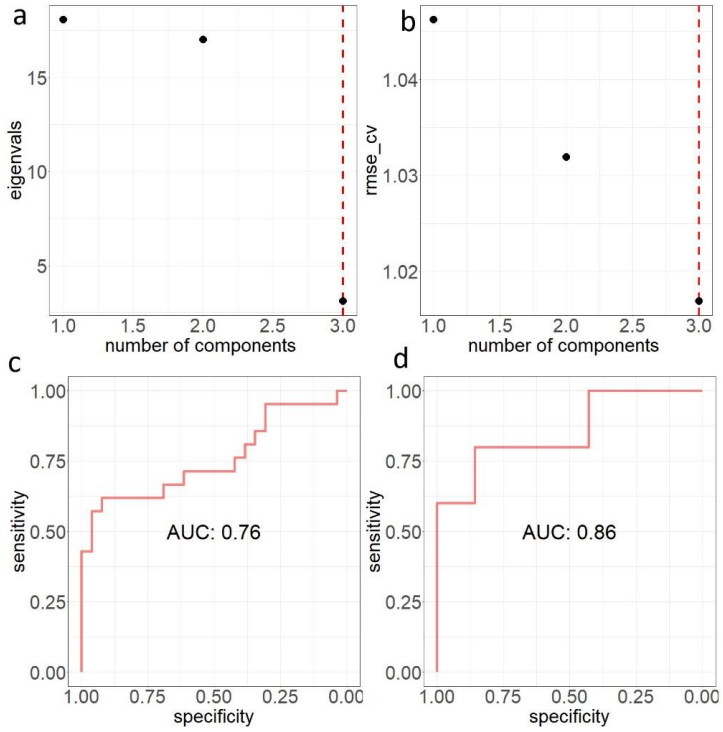

Fig. 2 Characteristics of the discrimination model for melanoma tissues of different invasions for one iteration of dividing the base into training and test sets. (a) Eigenvalues of loading vectors; (b) dependence of the mean square error of the model during cross-validation on the number of loading vectors; (c) characteristics of the constructed discrimination for the training sample; (d) characteristics of discrimination for the test sample.

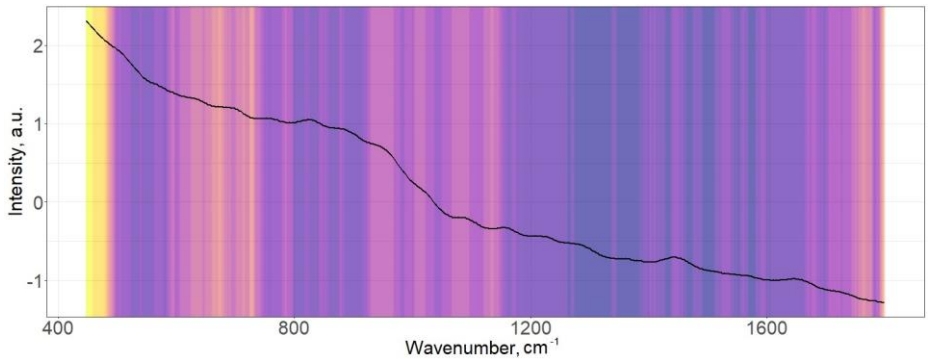

Fig. 3 VIP-distribution of spectrum variables in constructing discrimination of melanoma tissues by the degree of invasion (average result for 10 iterations of model construction).

As follows from Fig. 3, the most significant for the model is the spectrum intensity in the ranges of 450–500 cm^{-1}, 700–770 cm^{-1}, and 1070–1190 cm^{-1}. The greatest spectral contribution to the selected areas is made by the autofluorescent component. The main tissue fluorophores, such as elastin, collagen and NADH, are characterized by fluorescence when excited in the UV or short-wave visible range, whereas the main endogenous fluorophore of melanoma tissue, excited in the near-IR range, is melanin [24, 25]. Moreover, near-IR radiation penetrates tissue well, which allows obtaining information about the deep layers of the skin and pathologically associated changes in them. Therefore, a significant contribution of the autofluorescent component to the model may be due to an increase in the volume fraction of melanocytes with an increase in the stage of invasion and, as a consequence, an increase in the autofluorescent contribution associated with melanin [30]. The most informative areas of the Raman component for the constructed discrimination of melanoma tissues by the degree of invasion are the bands of 1385 cm^{-1}, 1445 cm^{-1}, 1487 cm^{-1}, 1565 cm^{-1}, and 1695 cm^{-1}. In general, peaks in these ranges indicate the presence of pigments (melanin), protein components (e.g., amide bonds, collagen), and lipid structures. Their combination and intensity may indicate characteristic features of melanoma tissue, such as high pigmentation concentration, altered protein structure, and increased metabolic activity. The 1385 cm^{-1} band may be associated with the spectral contribution of amines, nitrogen-containing groups, and amino acids, as well as melanin [31]. The 1445 cm^{-1} band is characteristic of $\delta(CH_2)$ and $\delta(CH_3)$ deformation vibrations in proteins and lipids, as well as amino acids and pigments [32]. This peak is often associated with protein and lipid components of tissues. The Raman band at 1487 cm^{-1} may be associated with pigments such as melanin, as well as carbon-carbon bonds in aromatic systems (e.g., amino acid residues or pigments) [33]. The peak in the 1487 cm^{-1} region may be associated with vibrations of amino acids such as tryptophan or tyrosine, which are important for the synthesis of melanin. This may indicate the activity of metabolic processes associated with pigment formation. The spectral contribution to the 1565 cm^{-1} band is characteristic of pigments, in particular melanin, as well as C=N bonds, which are present in some proteins and pigments [31]. The 1695 cm^{-1} band is associated with amide groups (amide I), characteristic of proteins, in particular with the C=O bond in the alpha-helical structure of the protein; it may also indicate the presence of collagen or other structural proteins [33]. The information content of the highlighted Raman bands for the constructed discrimination is lower relative to the information content of the autofluorescence component. However, taken together, both the autofluorescence component and the Raman component of the spectrum provide the construction of a stable model of discrimination of melanoma tissues by the degree of invasion. To date, the main method of analyzing melanoma invasion is histological analysis [34]. The degree of melanoma invasion Clark level in combination with other criteria, such as Breslow thickness, determined by an experienced pathologist based on histology, is an important prognostic factor for survival and the dynamics of the course of melanoma [35, 36]. The simplicity and availability of classical histological assessment, good clinical confirmation, and the possibility of standardized assessment ensure the widespread use of histology for determining the Clark level. At the same time, the methods of invasion analysis according to Clark, based on histological assessment, require high qualification of a specialist and are associated with possible subjectivity in determining the boundaries of invasion. Modern technologies and additional methods help to increase the accuracy and objectivity of histological assessment of melanoma invasion, which is important for determining the prognosis and choosing treatment tactics for melanoma. For example, the scientific group of M. Prodan et al. [37] and the team of authors Y. Li et al. [38] studied the prognostic significance of gene expression and markers in the analysis of invasiveness and progression of melanoma. Gene and biomarker expression is a powerful tool for assessing the invasiveness and progression of melanoma, allowing to predict tumor aggressiveness, the risk of metastasis, the effectiveness of therapy, and the likelihood of relapse.

It should be noted that melanoma progression is also associated with changes in the arrangement of collagen fibers in the skin. In the work [39], Sean J. Kirkpatrick et al. used the optical elastography method to study the mechanical properties of tissues that correlate with varying degrees of dermal damage by the neoplasm. Thus, the use of various methods for the analysis of melanoma invasion allows not only for more accurate assessment of the stage and risk of metastasis but also helps to better understand the pathological features of melanoma associated with its invasion, which contributes to the development of new therapeutic strategies. Spectral methods can be used for rapid noninvasive analysis of molecular and chemical changes in melanoma tissues of varying invasion, which is inaccessible with traditional histology.

The current study describes for the first time the investigation of the capabilities of spectral analysis based on Raman scattering and autofluorescence analysis for discrimination of melanoma tissues by the degree of invasion. The obtained results demonstrated the prospects for using spectral analysis for noninvasive determination of the degree of melanoma invasion and detection of pathologically associated changes in the component composition of melanoma tissues depending on the degree of invasion. At the next stage of the research, it is planned to increase the sample size of patients in order to build a stable regression between the spectral characteristics of melanoma tissue and the corresponding Clark level.

4 Conclusion

The presented results demonstrate that conventional Raman spectroscopy may be utilized for the in vivo evaluation of Clark level of invasion. The achieved accuracy of 75% for discrimination of I–II vs. III–V levels of invasion allows us to hope for the subsequent successful development of the approach with the subsequent possibility of more accurate determination of the invasion level. In this study we analyzed a limited dataset of Raman spectra from melanomas of different invasion levels, and in future studies the number of analyzed melanoma samples as well as the number of analyzed Raman spectra should be significantly increased (according to clinical procedures limitations, we were able to register only one Raman spectrum per analyzed melanoma sample). The proposed approach may be useful in the evaluation of a patient's prognosis. Moreover, as the registration and analysis of Raman spectra takes a couple of minutes, the evaluation of the patient's prognosis may be performed right on the first screening along with the determination of the neoplasm type based solely on the analysis of Raman spectra. Such an approach will save the time of the analysis and ultimately help the doctor to find the best treatment plan for the patient.

Disclosures

All authors declare that there is no conflict of interests in this paper.

Acknowledgments

This study is supported by R & D "Development of a hardware and software complex for non-invasive diagnostics of neoplasms using YERG-2023-0001 spectroscopy" within the framework of the State Order.

References

1. "Cancer Facts & Figures 2025," American Cancer Society, Atlanta (accessed 4 August 2025). [https://www.cancer.org/content/dam/cancer-org/research/cancer-facts-and-statistics/annual-cancer-facts-and-figures/2025/2025-cancer-facts-and-figures-acs.pdf].
2. D. Barh, A. Carpi, M. Verma, and M. Gunduz (Eds.), Cancer Biomarkers: Minimal and Noninvasive Early Diagnosis and Prognosis, CRC Press, Boca Raton (2017). eBook ISBN: 9780429169304.
3. M. Antohe, A. Coman, G. Turcu, R. I. Nedelcu, A. Brinzea, M. Balaban, A. Moroianu, L. Manea, I. Hulea, E. Balasescu, S. A. Zurac, M. Cioplea, C. Popp, L. Nichita, and D. A. Ion, "The prognostic significance of the clinical and histological parameters in primary cutaneous melanoma patients," Medicine and Pharmacy Reports 95(3), 229–235 (2022).
4. W. H. Clark, L. From, E. A. Bernardino, and M. C. Mihm, "The histogenesis and biologic behavior of primary human malignant melanomas of the skin," Cancer Research 29(3), 705–727 (1969).
5. K. Stawarz, A. Galazka, M. Misiak-Galazka, M. Durzynska, A. Gorzelnik, K. Bienkowska-Pluta, J. Korzon, F. Kissin, and J. Zwolinski, "Advances in skin ultrasonography for malignant and benign tumors of the head and neck: current insights and future directions," Journal of Clinical Medicine 14(7), 2298 (2025).
6. M. Kawaguchi, H. Kato, Y. Noda, K. Kobayashi, T. Miyazaki, F. Hyodo, and M. Matsuo, "Imaging findings of malignant skin tumors: radiological–pathological correlation," Insights Imaging 13(1), 52 (2022).
7. C. Burnette, T. E. Sivesind, and R. Dellavalle, "From the cochrane library: optical coherence tomography for diagnosing skin cancer in adults," Journal of Medical Internet Research Dermatology 6, e41355 (2023).
8. M. Zafar, A. P. Siegel, K. Avanaki, and R. Manwar, "Skin imaging using optical coherence tomography and photoacoustic imaging: a mini-review," Optics 5(2), 248–266 (2024).
9. F. S. L. Quintana, H. L. D. Almeida Jr., C. P. Ruas, and V. M. Jorge, "Scanning electron microscopy of dermatofibroma," Anais Brasileiros de Dermatologia Journal 94(3), 358–360 (2019).
10. Y. Ouyang, Y. Liu, Z. M. Wang, Z. Liu, and M. Wu, "FLIM as a promising tool for cancer diagnosis and treatment monitoring," Nano-Micro Letters 13(1), 133 (2021).
11. L. Rey-Barroso, S. Peña-Gutiérrez, C. Yáñez, F. J. Burgos-Fernández, M. Vilaseca, and S. Royo, "Optical technologies for the improvement of skin cancer diagnosis: A review," Sensors 21(1), 252 (2021).
12. D. Lunter, V. Klang, D. Kocsis, Z. Varga-Medveczky, S. Berkó, and F. Erdő, "Novel aspects of Raman spectroscopy in skin research," Experimental Dermatology 31(9), 1311–1329 (2022).
13. L. Franzen, M. Windbergs, "Applications of Raman spectroscopy in skin research − From skin physiology and diagnosis up to risk assessment and dermal drug delivery," Advanced Drug Delivery Reviews 89, 91–104 (2015).
14. I. A. Bratchenko, L. A. Bratchenko, A. A. Moryatov, Y. A. Khristoforova, D. N. Artemyev, O. O. Myakinin, A. E. Orlov, S. V. Kozlov, and V. P. Zakharov, "In vivo diagnosis of skin cancer with a portable Raman spectroscopic device," Experimental Dermatology 30(5), 652–663 (2021).
15. C. Delrue, R. Speeckaert, M. Oyaert, S. De Bruyne, and M. M. Speeckaert, "From vibrations to visions: raman spectroscopy's impact on skin cancer diagnostics," Journal of Clinical Medicine 12(23), 7428 (2023).
16. V. Mieites, M. G. Fernández-Manteca, I. Santiuste Torcida, F. Madrazo Toca, M. J. Marín Vidalled, and O. M. Conde, "Assessment of blood serum stability with Raman spectroscopy and explanatory AI," Spectrochimica Acta Part A: Molecular and Biomolecular Spectroscopy 340, 126297 (2025).

17. W. Liu, Z. Sun, J. Chen, and C. Jing, "Raman spectroscopy in colorectal cancer diagnostics: comparison of PCA-LDA and PLS-DA models," Journal of Spectroscopy 2016, 1–6 (2016).
18. J. Zhao, H. Lui, S. Kalia, T. K. Lee, and H. Zeng, "Improving skin cancer detection by Raman spectroscopy using convolutional neural networks and data augmentation," Frontiers in Oncology 14, 1320220 (2024).
19. S. Kucheryavskiy, "mdatools – R package for chemometrics," Chemometrics and Intelligent Laboratory Systems 198, 103937 (2020).
20. L. A. Bratchenko, Y. A. Khristoforova, I. A. Pimenova, E. N. Tupikova, M. A. Skuratova, G. A. Dvoynikov-Sechnoy, S. Wang, P. A. Lebedev, and I. A. Bratchenko, "SERS-based technique for accessible and rapid diagnosis of multiple myeloma in blood serum analysis," Light: Advanced Manufacturing 6(2), 284–294 (2025).
21. L. A. Bratchenko and I. A. Bratchenko, "Avoiding overestimation and the "black box" problem in biofluids multivariate analysis by raman spectroscopy: interpretation and transparency with the SP-LIME algorithm," Journal of Raman Spectroscopy 56(4), 353–364 (2025).
22. D. Wu, A. Fedorov Kukk, R. Panzer, S. Emmert, and B. Roth, "In vivo Raman spectroscopic and fluorescence study of suspected melanocytic lesions and surrounding healthy skin," Journal of Biophotonics 17(8), e202400050 (2024).
23. L. A. Bratchenko, Y. A. Khristoforova, A. A. Moryatov, and I. A. Bratchenko, "Raman spectroscopy based diagnosis of dermatofibrosarcoma protuberans: Case report," Photodiagnosis and Photodynamic Therapy 35, 102351 (2021).
24. S. Wang, J. Zhao, H. Lui, Q. He, and H. Zeng, "In vivo near-infrared autofluorescence imaging of pigmented skin lesions: methods, technical improvements and preliminary clinical results," Skin Research and Technology 19(1), 20–26 (2013).
25. S. Kalia, J. Zhao, H. Zeng, D. McLean, N. Kollias, and H. Lui, "Melanin quantification by in vitro and in vivo analysis of near-infrared fluorescence," Pigment Cell & Melanoma Research 31(1), 31–38 (2018).
26. P. T. Tran, P. Tawornchat, B. Kleuser, S. B. Lohan, J. Schleusener, M. C. Meinke, and M. E. Darvin, "Red- and near-infrared-excited autofluorescence as a marker for acute oxidative stress in skin exposed to cigarette smoke Ex Vivo and In Vivo," Antioxidants 12(5), 1011 (2023).
27. M. Emanuelli, D. Sartini, E. Molinelli, R. Campagna, V. Pozzi, E. Salvolini, O. Simonetti, A. Campanati, and A. Offidani, "The double-edged sword of oxidative stress in skin damage and melanoma: From physiopathology to therapeutical approaches," Antioxidants 11(4), 612 (2022).
28. M. Pietruszewska, G. Biesiada, J. Czepiel, M. Birczyńska, P. Moskal, M. Kozicki, E. Hola, A. Garlicki, and A. Wesełucha-Birczyńska, "Lymphocytes studied by Raman microspectroscopy," Chapter 6 in Lymphocytes, E. S. Istifli, H. B. İla (Eds.), IntechOpen (2019). eBook ISBN: 978-1-83881-749-7.
29. M. Pietruszewska, G. Biesiada, J. Czepiel, M. Birczyńska-Zych, P. Moskal, A. Garlicki, and A. Wesełucha-Birczyńska, "Raman spectroscopy of lymphocytes from patients with the Epstein–Barr virus infection," Scientific Reports 14(1), 6417 (2024).
30. W. H. Clark, "From the melanocyte to melanoma to tumor biology," Advances in Cancer Research 65, 113–140 (1194).
31. Z. Huang, H. Lui, X. K. Chen, A. Alajlan, D. I. McLean, and H. Zeng, "Raman spectroscopy of in vivo cutaneous melanin," Journal of Biomedical Optics 9(6), 1198 (2004).
32. B. R. Uslu, B. Ozdil, E. Tarhan, S. Özçelik, H. Aktuğ, and G. Güler, "Vibrational spectroscopy unveils distinct cell cycle features of cancer stem cells in melanoma," Scientific Reports 15(1), 28494 (2025).
33. Z. Movasaghi, S. Rehman, and I. U. Rehman, "Raman spectroscopy of biological tissues," Applied Spectroscopy Reviews 42(5), 493–541 (2007).
34. W. H. Clark, D. E. Elder, and M. Van Horn, "The biologic forms of malignant melanoma," Human Pathology 17(5), 443–450 (1986).
35. A. A. Marghoob, K. Koenig, F. V. Bittencourt, A. W. Kopf, and R. S. Bart, "Breslow thickness and Clark level in melanoma: Support for including level in pathology reports and in American joint committee on cancer staging," Cancer 88(3), 589–595 (2000).
36. O. Vița, A. Jurescu, A. Văduva, R. Cornea, M. Cornianu, S. Tăban, D. Szilagyi, C. Micșescu, B. Natarâș, and A. Dema, "Invasive cutaneous melanoma: Evaluating the prognostic significance of some parameters associated with lymph node metastases," Medicina 59(7), 1241 (2023).
37. M. Prodan, S. Costescu, A. Elagez, S. M. D. Laitin, V. Bloanca, Z. Crainiceanu, E. Seclaman, A.-O. Toma, R. M. Fericean, G. Puenea, and G. V. Cozma, "Molecular markers in melanoma progression: A study on the expression of miRNA gene subtypes in tumoral vs. benign nevi," Current Oncology 31(5), 2881–2894 (2024).
38. Y. Li, J. M. Krahn, G. P. Flake, D. M. Umbach, and L. Li, "Toward predicting metastatic progression of melanoma based on gene expression data," Pigment Cell & Melanoma Research 28(4), 453–463 (2015).
39. S. J. Kirkpatrick, R. K. Wang, D. D. Duncan, M. Kulesz-Martin, and K. Lee, "Imaging the mechanical stiffness of skin lesions by in vivo acousto-optical elastography," Optics Express 14(21), 9770 (2006).